Phase separating colloid polymer mixtures in shear flow

Didi Derks[1,2]**, Dirk G A L Aarts**[3]**, Daniel Bonn**[2,4] **and Arnout Imhof**[1]

[1] Soft Condensed Matter, Debye Institute, Utrecht University, Princetonplein 5,
3584 CC Utrecht, The Netherlands
[2] Laboratoire de Physique Statistique, Ecole Normale Supérieure, 24 rue Lhomond,
75231 Paris cedex 05, France
[3] Department of Chemistry, Physical and Theoretical Chemistry Laboratory,
Oxford University, South Parks Road, Oxford OX1 3QZ, UK
[4] van der Waals-Zeeman Institute, University of Amsterdam, Valckenierstraat 65,
1018 XE Amsterdam, The Netherlands

E-mail: didi.derks@lps.ens.fr

Abstract
We study the process of phase separation of colloid polymer mixtures in the (spinodal) two-phase region of the phase diagram in shear flow. We use a counter-rotating shear cell and image the system by means of confocal laser scanning microscopy. The system is quenched from an initially almost homogeneous state at very high ($200 \, \text{s}^{-1}$) shear rate to a low shear rate $\dot{\gamma}$. A spinodal decomposition pattern is observed. Initially, the characteristic length scale increases linearly with time. As the structure coarsens, the shear imposes a certain length scale on the structure and a clear asymmetry develops. The domains become highly stretched along the flow direction, and the domain width along the vorticity axis reaches a stationary size, which scales as $\approx \dot{\gamma}^{-0.35}$. Furthermore, on quenching from an intermediate ($6.7 \, \text{s}^{-1}$) to a low shear rate the elongated structures become Rayleigh unstable and break up into smaller droplets. Still, the system eventually reaches the same steady state as was found from a direct high to low shear rate quench through coarsening.

1. Introduction

When an initially homogeneous mixture is quenched into the spinodal regime complex patterns are observed during the ensuing fluid–fluid phase separation. Understanding the morphology and its kinetics requires answering questions of both hydrodynamic and thermodynamic nature, and is therefore interesting from a fundamental point of view. It has consequently been the subject of many studies, see for example [1–3]. Qualitatively different morphologies and kinetics are observed when the system is kept in a nonequilibrium state by continuous driving, such as a shear flow. Phase transitions of fluids in shear flow have been reviewed in [4] and [5]. Insight in the demixing behavior, especially in flow, is also of importance in for example the food industry [6] and polymer processing [7].

The kinetics of spinodal decomposition of liquid mixtures and polymer blends under shear has been studied by means of light scattering and rheology [8–11]. These studies have shown that domain growth in the flow direction is enhanced by the shear, leading to an anisotropic domain structure. Using microscopy, Hashimoto and co-workers observed extreme elongation at high shear in phase separating polymer–polymer solutions, which they termed 'string phase'. The diameter of a string was reported to decrease with increasing shear rate [11]. Upon further increasing the shear rate, the diameter of these strings approached the interface thickness, at which point the system became homogeneous again [12]. An open question is whether at fixed shear rate domain growth will continue indefinitely as in zero shear, or whether a steady state is eventually reached.

To investigate the existence of steady states, Cates and co-workers recently performed Lattice Boltzmann simulations of binary mixtures undergoing phase separation [13, 14]. In both 2D [13] and 3D [14], shear was seen to suppress macroscopic phase separation and evidence was found for a nonequilibrium

steady state consisting of a bicontinuous structure, in which the domains were stretched in the flow direction.

In the present work a colloid polymer mixture is used to study phase separation under shear. Such mixtures display a rich phase behavior including a coexistence between a colloidal gas phase (poor in colloids, rich in polymers) and a colloidal liquid phase (rich in colloids, poor in polymers). This phase separation occurs at high enough colloid and polymer concentrations, and originates from an effective (depletion) attraction between the colloidal spheres caused by the polymers [15, 16]. The process of phase separation at rest in such mixtures was studied by both small angle light scattering (SALS) [17] and microscopy [17, 18].

It was found that the initial stage of demixing is driven by diffusion of individual particles. Since a homogeneous system is unstable in the two-phase region of the phase diagram each density fluctuation will have a lower free energy than the initial state and will thus tend to grow further. However, not all wavelength fluctuations grow at the same rate, and a fastest growing mode exists, which produces the characteristic length scale of a spinodal structure. With SALS the early stages of phase separation can be accessed [17], while microscopy is very suited to study the interfacial tension driven coarsening which immediately follows, after the interfaces have formed on a microscopic scale. As the structures grow larger, gravity drives the demixing further, leading to the formation of a macroscopic interface [18].

In this paper we focus on the phase separation in shear flow of the same colloid–polymer mixture that was used in [18]. First, we describe experiments in which the mixture was brought into a nearly homogeneous state by application of a high shear rate and investigate the demixing upon quenching to a lower shear rate. The development of the structures was followed in time and compared to experiments in absence of shear. Second, we consider what happens after a sudden shear rate change, when the system is initially in an inhomogeneous steady state.

2. Experimental details

We used poly-(methylmethacrylate) (PMMA) spheres with a diameter of 50 nm (polydispersity < 10%). They were fluorescently labeled with 7-nitrobenzo-2-oxa-1,3,-diazole (NBD). As polymer we used polystyrene with a radius of gyration of 14 nm ($M_w = 2 \times 10^5$ g mol^{-1}) [19]. The samples were prepared by mixing stock dispersions of colloids and of polymer, each of which was dispersed in decalin. The resulting colloid and polymer volume fractions in the mixture were $\phi_c = 0.076$ and $\phi_p = 0.50$, respectively. At these concentrations the mixture is in the two-phase region of the phase diagram, reasonably close to the critical point [20]. After phase separation the volumes of the two phases are roughly equal.

At this state point the system is characterized by an interfacial tension of 2×10^{-7} N m^{-1} and a density difference of 0.053 g ml^{-1} as was found by analyzing the thermally induced capillary waves at a freely fluctuating interface [21]. The viscosity was measured by performing rheology experiments on both phases separately, and turned out to be 8 mPa s for the gas phase and 31 mPa s for the liquid phase [18].

To study the phase separating system under shear a home built counter-rotating shear cell was used. This cone-plate shear cell is placed on top of a confocal microscope (Leica TCS SP2) which is used in fluorescence mode (excitation wavelength 488 nm). The colloidal liquid, which contains a high concentration of fluorescent colloids will appear bright, while the colloidal gas phase is darker since the colloid concentration in it is lower. The counter-rotating principle of the shear cell allows us to locate the zero-velocity plane in the bulk of the cell, where the observations are carried out. We refer to [22] for further details on the shear cell. In this setup the velocity gradient ∇ is directed along the vertical axis (z), parallel to gravity. The flow (x) and vorticity (y) directions lie in the horizontal plane. Unless stated otherwise, the images shown are taken in this flow-vorticity plane. A long working distance 20 × 0.7 NA objective was used in order to have a large field of view (750 × 750 μm^2).

The sample was homogenized (hand shaken) and then brought onto the glass plate of the shear cell. The cone was then mounted onto the set up, and brought into measuring position. Immediately after that a high shear rate of 200 s^{-1} was applied.

3. Coarsening in the presence of shear

3.1. Quenches from high to low shear rate

We applied a high shear of 200 s^{-1}, homogenizing the mixture, and then followed the process of phase separation after a sudden decrease of the shear rate. The shear cell achieves this drop in about 1 s. Here we first discuss a quench from this high shear rate to no shear at all. A time series was taken immediately after cessation of the shear. In figures 1(a)–(f) snapshots are shown taken in the first 40 s after the quench. The system is seen to undergo a spinodal decomposition, where a continuous structure coarsens in time. These micrographs do not make it possible to determine whether the system was fully homogenized before the shear rate quench. However, it probably was not, since just after the quench the structures are already slightly larger in the flow direction then in the vorticity direction. In time, the system is seen to become more and more isotropic, displaying a typical spinodal structure.

In figures 1(g)–(l) snapshots of a similar quench are shown, but now the final shear rate is 2.7 s^{-1}. The first few seconds the structures resemble the result above, but after about 20 s the shear is seen to drastically deform the structure into domains that are elongated in the flow direction. By imaging vertical cross sections (flow-gradient plane) we observed that the structures are approximately cylinder-shaped, with two short dimensions (in the vorticity and gradient direction) and one long dimension, along the flow axis (see figure 6). Interestingly, after about 30 s the characteristic length scales in the image appear to remain unaltered, even though the details of the domain structure keep changing continuously. This last observation applies especially to the vorticity direction.
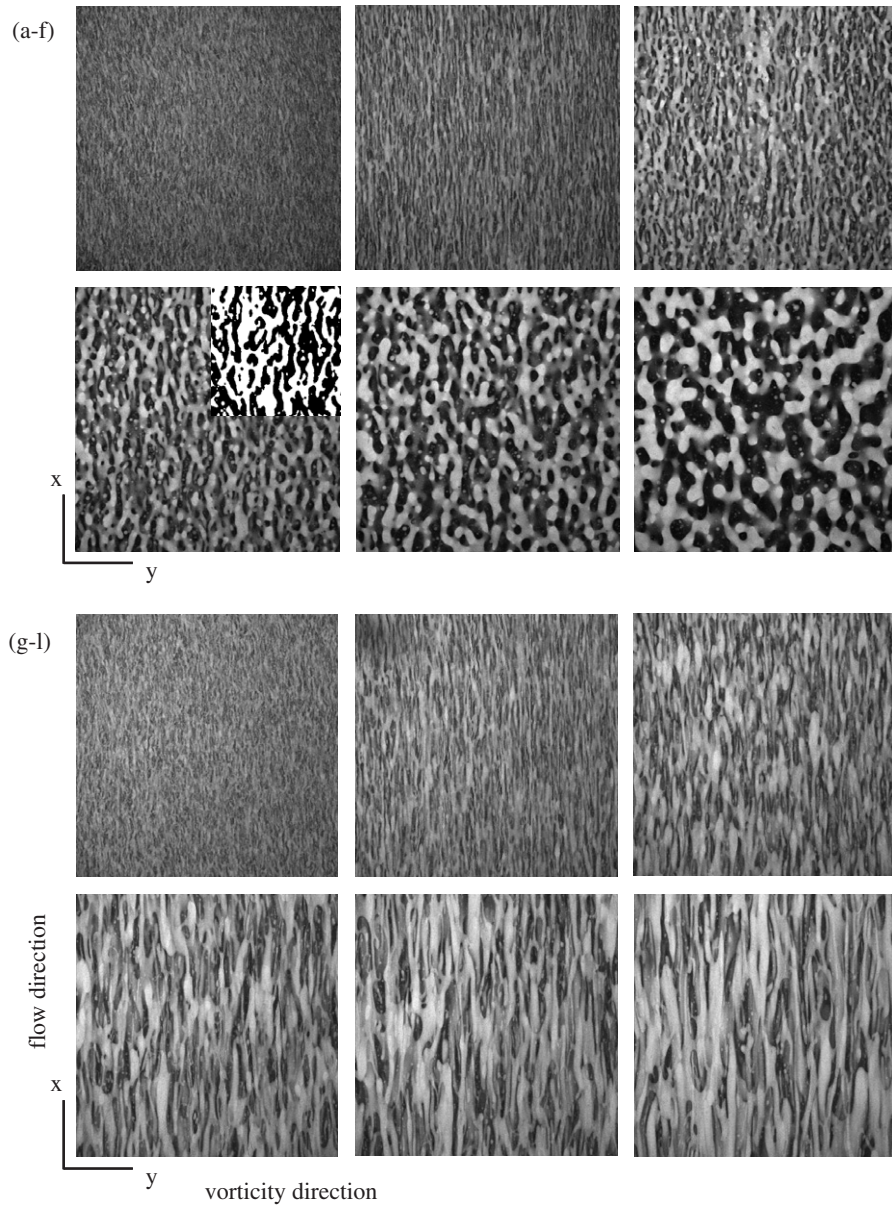
Figure 1. Time series showing the process of the demixing after a sudden drop of the shear rate from 200 s^{-1} to no shear ((a)–(f)), and to a shear rate of 2.7 s^{-1} ((g)–(l)) at $t = 0$ s. Image size is 750×750 μm^2. Snapshots correspond to $t = 6.6$ s ((a), (g)), 9.8 s ((b), (h)), 16.4 s ((c), (i)), 21.3 s ((d), (j)), 27.9 s ((e), (k)), and 37.7 s ((f), (l)). The inset in (d) displays part of the image after binarization.

For this reason, we focus in our analysis on the domain size in the vorticity direction. We obtain the typical size directly by binarizing the images: when the intensity of a point is below the average intensity of that image, it is said to belong to the gas phase; when it is above this threshold it is taken to be part of the liquid phase. The inset in figure 1(d) shows an example of such a binarization. Since the contrast between the phases is sufficiently large, the binarized image reproduces the domain structure well. Subsequently, we determine in each frame the average number of times an interface is crossed in going from the left to the right. By doing this for every horizontal cross-section we obtain the average domain size as a function of time (figure 2(b)).

Alternatively, the coarsening rate of phase separation can be found by performing a Fourier transformation (FFT) of confocal images, as was done in [18]. This method is analogous to what would be measured in a scattering experiment [17]. The typical size is then obtained from the wavenumber k_{max} at the maximum of the power spectrum as shown in figure 2(a).

Both the FFT and the binarization method give similar results, as is shown in figure 2(b) where L_y is defined as the length for the whole period of a fluctuation (that is, including a gas and a liquid domain). We find a linear time dependence of the typical structure size, confirming that the coarsening is interfacial tension driven. Moreover, we find that the coarsening rate, obtained from the slope of the graph, is 1.5–2 μm s^{-1}. This is in agreement with expectations for a sample with this interfacial tension and viscosity as discussed in detail in [18].
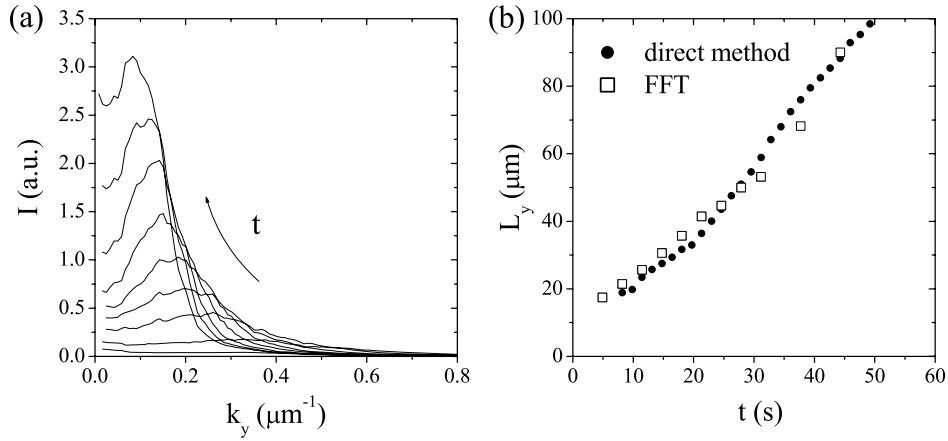
Figure 2. (a) Analysis of the growth of the characteristic domain size along the vorticity axis of the spinodal structure, which develops after a shear quench from high to zero shear rate (see figure 1). (b) Both the method using the power spectrum of a Fourier transform and a direct binarization method, in which the number of interfaces along the vorticity direction is counted, lead to a similar curve.
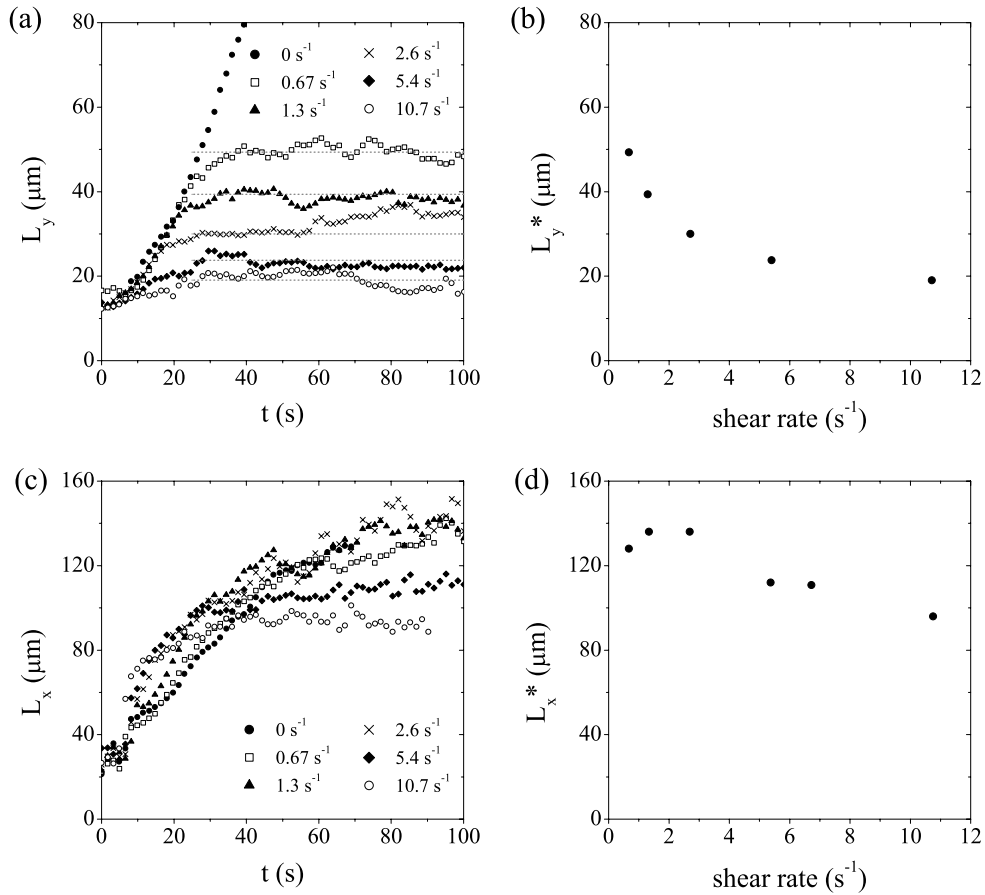

Figure 3. ((a), (c)) Evolution of the characteristic length of the spinodal structure along the vorticity axis (a) and the flow axis (c), which develops after a quench from high (200 s^{-1}) to low shear rate. ((b), (d)) Final values of L_y and L_x after a steady state had been reached.

We use the same binarization method to follow the evolution of the typical domain size in both vorticity and flow direction in shear flow. From figure 3 the difference between the sheared and non-sheared case becomes clear. While in the sheared systems the domain size initially also increases (linearly) in time, the size eventually levels off to a constant value. This plateau value is seen to become lower as the shear rate is increased (figures 3(a) and (c)). The gradual change with

shear rate from an isotropic structure all the way to very thin threads is visualized in figure 4, in which we show snapshots taken after the plateau value had been reached.

3.2. Quenches from intermediate shear rate

Apart from quenching from an initially almost homogeneous state, we can also start at an intermediate shear rate in
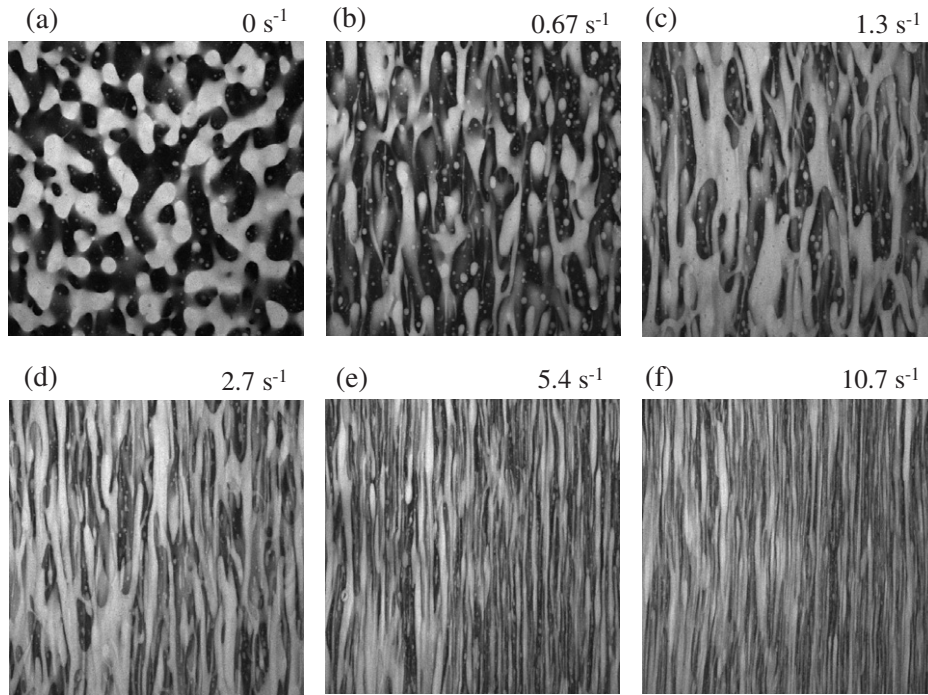
Figure 4. Snapshots taken 50 s after quenching the system to the shear rate shown. All these images show a steady state, except for the quench to zero shear (a), where in the absence of shear flow the structure continues to coarsen. Image size is $750 \times 750 \ \mu\mathrm{m}^2$.

which elongated domains have already been established. In figure 5 we show an example of such an experiment, where we start with bands that are on average 21 μm wide. The process clearly shows qualitatively different kinetics than in the previous quenches: thin bands that were initially stable at a shear rate of 6.7 s^{-1}, are seen to quickly break up into small droplets after the quench (figures 5(a)–(e)). Wider structures remain intact for longer times, but eventually develop instabilities as well, giving them a more tortuous appearance and sometimes causing breakup (figures 5(f) and (g)). These instabilities are also observed in the flow-gradient plane, as is shown in figure 6.

When the system coarsens further, most small droplets are absorbed into a new continuous structure and the system reaches a steady state again (figures 5(h)–(j)). Interestingly, the domain structure looks quite similar to that resulting from a direct quench from a high shear rate (compare with figure 4(b)), and indeed the final domain width we obtain in this way is identical; see figure 7. Moreover, when the shear rate is now increased again, as indicated by the arrows, the final size still falls exactly on the same curve. From this we conclude that shear flow drives the system to a unique steady state, although the path that is taken to get there can be very different.

Figure 7 summarizes our results and shows that the width of domains along the vorticity axis scales as $\approx \dot{\gamma}^{-0.35}$. Here, the filled circles refer to the quench experiments discussed in section 3.1. We also indicated the shear rate of 200 s^{-1} from which we quenched. By extrapolating our results to this high shear rate, we can estimate that the typical size expected in the initial structure was $\sim$7 μm, just one order of magnitude larger

then the interface width, which is the criterion for complete homogenization [12].

4. Discussion

In general, the initial stage of phase separation is driven by thermodynamics and controlled by diffusion. In this regime a typical density fluctuation of size L diffuses in a time $t \propto L^2/D$. Here D is its diffusion coefficient, which according to the Stokes–Einstein relation is given by ratio of the thermal energy $k_B T$ and the drag coefficient $f \propto \eta L$, with η the viscosity. Since the drag coefficient in itself is also proportional to the size, the typical size of a density fluctuation initially grows as [1, 2]:

$$L \propto \left(\frac{k_B T}{\eta} \right)^{1/3} t^{1/3}. \tag{1}$$

As time proceeds the system develops a sharper and sharper interface, with an interfacial tension approaching its equilibrium value σ. It turns out that particles have to diffuse only over a distance on the order of the final interface thickness ($L \propto \sqrt{k_B T/\sigma} \sim \xi$) to develop such an interface. From then on capillary forces will drive further coarsening, lowering the free energy by reduction of the total interfacial area. The cross-over occurs typically already when the structure size is on the order of micrometers, which is the reason why our microscopy experiments only provide access to the interfacial tension driven regime and not the diffusive regime.

The coarsening rate in the interfacial tension driven regime can be understood as follows. It is governed by the Stokes equations [2], and can be found by balancing, on one hand, the gradient in pressure over the curved surfaces (∇p) and, on
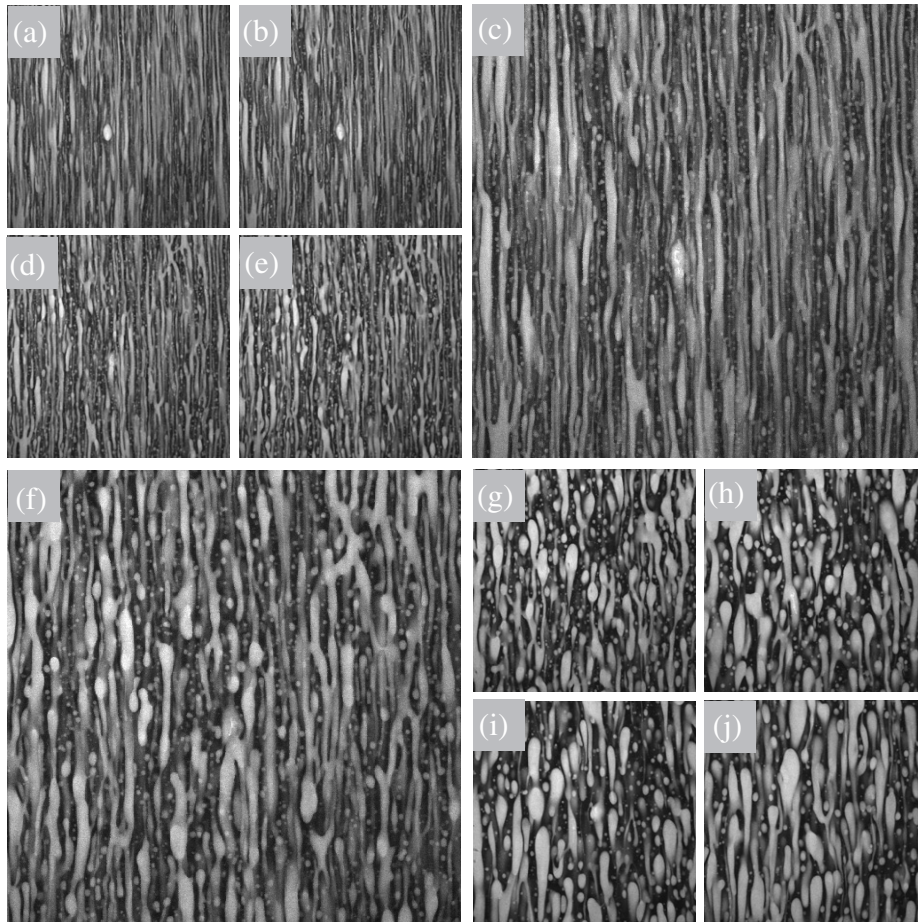
Figure 5. Structure evolution after an intermediate-to-low shear rate quench. At $t = 0$ s the shear is dropped from 6.7 to 0.67 s^{-1}. Subsequent images were taken at $t = 1.6$ s (b), 3.3 s (c), 6.6 s (d), 9.8 s (e), 13.1 s (f), 26.2 s (g), 39.4 s (h), 52.5 s (i) and 78.7 s (j).
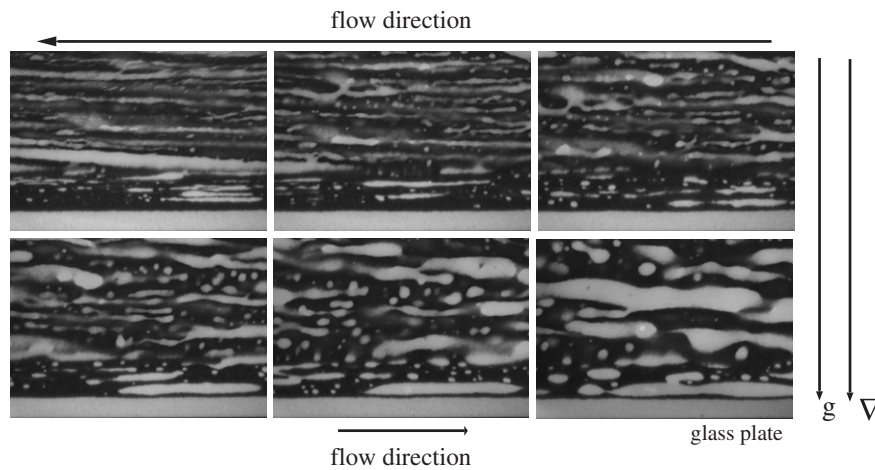

Figure 6. Snapshots in the flow-gradient plane after a quench from high (66 s^{-1}) to a shear rate of 1.3 s^{-1}. Images are taken with 63× oil-immersion objective. Image width is 132 μm; image height is $\sim$92 μm.

the other hand, the viscous dissipation ($\eta \nabla^2 \vec{u}$). Within each phase the difference in Laplace pressure between concave and convex regions is of order σ/L. As those regions are typically a distance L apart, the gradient is well approximated by $1/L$. Similarly, the dissipation term can be estimated from the size of the structure L, resulting in:

$$|\nabla p| \propto \frac{1}{L}\frac{\sigma}{L} \qquad \text{and} \qquad \eta \nabla^2 u \propto \eta \frac{1}{L^2} u. \qquad (2)$$

From this we see that, in absence of shear flow, a constant coarsening rate $u_{cap} \propto \sigma/\eta$ is expected: $L \propto (\sigma/\eta)t$.
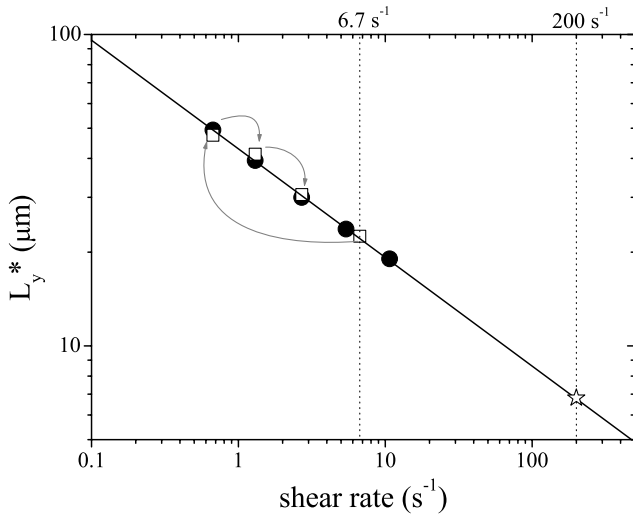
Figure 7. The plateau value to which the typical domain size along the vorticity direction levels off scales as $\dot{\gamma}^{-1/3}$. (Solid circles) quench from 200 s^{-1}, (open squares) quench from 6.7 s^{-1}.

In this so-called *fast* hydrodynamic regime (as opposed to slow diffusive processes) the spinodal structure coarsens since mass flows rapidly within the two phases from high pressure (convex) regions to (concave) regions of lower pressure, thereby decreasing the interfacial area [23].

Our measurements show that, with a shear flow applied, domain coarsening in the vorticity direction takes place with the same growth rate as without shear. In the flow direction, on the other hand, the growth rate is enhanced by the shear (figures 3(a) and (c)). This result is in agreement with experiments on phase separation in molecular systems [8]. At later times the shear begins to strongly affect the spinodal structure also in the vorticity and gradient directions, and limits the size to which the domains can eventually grow. This situation represents a true steady state that is uniquely determined because the same state is reached when quenching from different initial shear rates, both above and below the final shear rate, at least to within the experimental uncertainty.

Can we understand at what length scale the shear becomes dominant? A simple hypothesis would be that this occurs as soon as the applied deformation rate $u_{\text{app}} = \dot{\gamma}L$ exceeds the capillary velocity u_{cap}. The rate with which shear tends to deform the domains increases as the structure coarsens while the capillary velocity is constant, and thus a cross-over is expected. Using similar scaling arguments as before, we can now write:

$$|\nabla p| \propto \frac{1}{L}\frac{\sigma}{L} \qquad \text{and} \qquad \eta\nabla^2 u \propto \eta\frac{1}{L^2}\dot{\gamma}L, \qquad (3)$$

leading to a domain width which scales as the inverse of the shear rate: $L \propto \sigma/\eta\dot{\gamma}$. This result is similar to the classical results of Taylor who studied the elongation of individual droplets suspended in a sheared liquid [23]. However, on the basis of our results we clearly have to reject this description as an explanation for the steady state domain size, which we find to scale as $L \propto \dot{\gamma}^{-0.35}$.

It is interesting to compare our microscopy experiments with those on demixing polymer–polymer solutions [11]. In this work, Hashimoto and co-workers found that the final domain size in the vorticity direction satisfies:

$$L_y^* \cong \frac{2\pi}{q_m(0)}\left(\dot{\gamma}\tau_\xi\right)^{-\alpha}, \qquad (4)$$

where $q_m(0)$ is the wavenumber of the fastest growing mode just after cessation of strong shear, τ_ξ is related to the growth rate of that mode, and $\alpha = 1/4$–$1/3$. The exponent is very similar to our result. Expression (4) was derived by Onuki [1, 4] by assuming a direct cross-over between the diffusive and the shear regime. This cross-over is for high viscosity systems as used in [11] more accessible. In our case, however, a competition between diffusion and shear would give rise to a length L which is typically only 1 μm, and as such more than an order of magnitude away from our experimental results. We therefore cannot offer a theoretical understanding of this result.

Interestingly, evidence for a nonequilibrium steady state was recently found in Lattice Boltzmann (LB) simulations. The domain sizes were found to scale approximately as $\dot{\gamma}^{-2/3}$, the exponents being slightly, but significantly, different for the three directions. Quantitative comparisons with the simulations of Stansell *et al* [13] and Stratford *et al* [14] fail in the sense inertia is important in their case. Our experiments take place at very low Reynolds numbers (Re $= \rho uL/\eta$ at most 0.01 for the largest domains); inertia is therefore not expected to be important in our case. Using two-dimensional numerical simulations of a different type Fielding [24] recently reproduced the LB results, and put forward an argument that for a steady state in a binary mixture to arise a competition between viscous and inertial regimes is required, since only that can explain the appearance of two different length scales. In simulations where inertia was strictly absent no steady state was found. It is as yet unclear how this can be reconciled with our experimental findings.

Furthermore, in our experiments a Rayleigh-type instability is observed upon lowering the shear rate from a previously steady state with elongated domains. First the thinnest domains break up into small droplets and then thicker ones do, but sufficiently thick domains somehow escape this fate. An alternative explanation for the stability of the highly elongated domain structure may therefore be sought in a stabilizing action of shear on liquid threads. Recent theory on isolated viscous threads has shown that under some conditions such an effect is indeed possible [25, 26]. The stability analysis is rather involved, but the physical picture behind it is relatively straightforward: without shear the only unstable mode on the cylinder is the axisymmetric varicose mode, which grows by the Rayleigh instability, due to differences in capillary pressure along the length of the thread. Other modes like the undulation, or higher order modes are stable. What shear will do is mix the unstable mode with the stable ones, resulting in a less unstable situation. In other words, an initial varicose fluctuation will be convected away, thereby reducing the pressure differences that make the instability grow. This could possibly lead to a stable string phase.

Such a phenomenon has not yet been demonstrated experimentally, however. Migler [27] did observe the appearance of stable threads in concentrated polymer blends above a critical shear rate, but showed that a necessary condition for their formation was a finite gap size of the shearing apparatus. In our setup the gap is 425 μm, reducing finite size effects. We should further note that we do not observe a 'true' string phase in which each string is stable. Instead, the stringlike domains form a continuous network structure and are highly dynamic, with individual strings continuously breaking up, reforming, and merging. A full explanation of our observations will therefore probably be considerably more complex.

5. Conclusion

The process of phase separation in colloid–polymer mixtures under shear was studied in real space by quenching the system from a high shear rate, where the system is almost homogeneous to a much lower shear rate. Initially, the domains are seen to grow linearly in time, as is typical in interfacial tension driven spinodal decomposition. The growth rate perpendicular to the flow does not depend on shear rate. As the domains grow larger there comes a point where the spinodal structure begins to be affected by the shear. The domains become highly stretched in the flow direction, while a stationary width is reached in the vorticity direction. This domain width is seen to scale as $\dot{\gamma}^{-0.35}$. Furthermore, we showed that this steady state is unique in the sense that it is independent of previous shear history, be it above or below the final rate. Notably, the kinetics in these two cases are rather different. In particular, when highly elongated domains are quenched to a lower shear rate the growth of the domain widths appears to be governed by a Rayleigh instability.

Acknowledgments

References

[1] Onuki A 2002 *Phase Transition Dynamics* (Cambridge: Cambridge University Press)
[2] Siggia E D 1979 *Phys. Rev.* A **20** 595
[3] Bray A J 1994 *Adv. Phys.* **43** 357
[4] Onuki A 1997 *J. Phys.: Condens. Matter* **9** 6119
[5] Han C C, Yao Y, Zhang R and Hobbie E K 2006 *Polymer* **47** 3271
[6] Lorén N, Alstkär A and Hermansson A M 2001 *Macromolecules* **34** 8117
[7] Tanaka H 2000 *J. Phys.: Condens. Matter* **12** R207
[8] Chan C K, Perrot F and Beysens D 1991 *Phys. Rev.* A **43** 1826
[9] Krall A H, Sengers J V and Hamano K 1992 *Phys. Rev. Lett.* **69** 1963
[10] Läuger J, Laubner C and Gronski W 1995 *Phys. Rev. Lett.* **75** 3576
[11] Hashimoto T, Matsuzaka K, Moses E and Onuki A 1995 *Phys. Rev. Lett.* **74** 126
[12] Fujioka K, Takebe T and Hashimoto T 1993 *J. Chem. Phys.* **98** 717
[13] Stansell P, Stratford K, Desplat J-C, Adhikari R and Cates M E 2006 *Phys. Rev. Lett.* **96** 085701
[14] Stratford K, Desplat J-C, Stansell P and Cates M E 2007 *Phys. Rev.* E **76** 030501
[15] Asakura S and Oosawa F 1954 *J. Chem. Phys.* **22** 1255
[16] Vrij A 1976 *Pure Appl. Chem.* **48** 471
[17] Verhaegh N A M, van Duijneveldt J S, Dhont J K G and Lekkerkerker H N W 1996 *Physica* A **230** 409
[18] Aarts D G A L, Dullens R P A and Lekkerkerker H N W 2005 *New J. Phys.* **7** 40
[19] Berry G C 1966 *J. Chem. Phys.* **44** 4550
[20] Aarts D G A L and Lekkerkerker H N W 2004 *J. Phys.: Condens. Matter* **16** S4231
[21] Aarts D G A L, Schmidt M and Lekkerkerker H N W 2004 *Science* **304** 847
[22] Derks D, Wisman H, van Blaaderen A and Imhof A 2004 *J. Phys.: Condens. Matter* **16** S3917
[23] Larson R G 1999 *The Structure and Rheology of Complex Fluids* (Oxford: Oxford University Press)
[24] Fielding S M 2008 *Phys. Rev.* E **77** 021504
[25] Frischknecht A 1998 *Phys. Rev.* E **58** 3495
[26] Gunawan A Y, Molenaar J and van de Ven A A F 2005 *Eur. J. Mech.* B **24** 379
[27] Migler K B 2001 *Phys. Rev. Lett.* **86** 1023